Estrogen promotes the metastasis of non-small cell lung cancer via estrogen receptor β by upregulation of Toll-like receptor 4 and activation of the myd88/NF-κB/MMP2 pathway

SHENG FAN[1], YONGDE LIAO[2], WENLIN QIU[3], QUANFU HUANG[2], HAN XIAO[2], CHANGYU LIU[3], DONG LI[3], XIAONIAN CAO[3], LEQUN LI[3], HUIFANG LIANG[4], BO AI[3] and SHENG ZHOU[5]

[1]Department of Thoracic Surgery, The First Affiliated Hospital of Xiamen University, Xiamen University, Xiamen, Fujian 361000; [2]Department of Thoracic Surgery, Xiehe Hospital, Tongji Medical College, Huazhong University of Science and Technology, Wuhan, Hubei 430022; [3]Department of Thoracic Surgery, [4]Hepatic Surgery Center, and [5]Department of Pathology, Tongji Hospital, Tongji Medical College, Huazhong University of Science and Technology, Wuhan, Hubei 430030, P.R. China

Received August 24, 2019; Accepted February 4, 2020

DOI: 10.3892/or.2020.7574

Abstract. Estrogen promotes non-small cell lung cancer (NSCLC) metastasis via estrogen receptor β (ERβ)-mediated invasiveness-associated matrix metalloprotease 2 (MMP2) upregulation. However, how ERβ increases the aggressiveness of NSCLC cells remains unclear. Recently, MMP2 was found to be upregulated by Toll-like receptor 4 (TLR4) signaling activation and to promote NSCLC metastasis. Our present study aimed to examine the role of ERβ in the activation of TLR4 signaling and in tumor progression and metastasis, and to explore the synergistic metastatic effect of a combination of ERβ and TLR4 activation on human NSCLC cells *in vitro* and *in vivo*. Here, we found that ERβ is associated with TLR4 in metastatic lymph nodes. Western blot analysis and immunofluorescence revealed that ERβ overexpression upregulated TLR4 protein expression and activated downstream targets, myeloid differentiation primary response 88 (myd88)/nuclear factor (NF)-κB/MMP2, enhancing NSCLC cell migration and invasion *in vitro*. A novel ERβ-TLR4 interaction in cell plasma was identified by co-immunoprecipitation and confocal immunofluorescence. The combination of estradiol and specific TLR4 agonist lipopolysaccharide (LPS) synergistically promoted metastatic behaviors in NSCLC cells. In cell culture and murine lung metastasis models, exposure to estradiol and LPS induced increased matrix degradation and accelerated invadopodia and metastasis formation in NSCLC cells compared with that in cells treated with estradiol or LPS alone. Together, we showed that estrogen promoted NSCLC metastasis via ERβ by upregulating TLR4 and activating its downstream signaling axis myd88/NF-κB/MMP2. The combined targeting of ERβ and TLR4 may be a novel therapeutic strategy against advanced metastatic lung cancer.

Correspondence to: Professor Yongde Liao, Department of Thoracic Surgery, Xiehe Hospital, Tongji Medical College, Huazhong University of Science and Technology, 1277 Jiefang Dadao Street, Wuhan, Hubei 430022, P.R. China
E-mail: liaotjxw@126.com

Key words: estrogen receptor β, Toll-like receptor 4, signaling pathway, non-small cell lung cancer, NSCLC, metastasis

Introduction

Non-small cell lung cancer (NSCLC) is one of the most common malignancies, leading in both the incidence and mortality rates worldwide (1). According to recent reports, metastatic NSCLC contributes to rising morbidity and underlies the majority of lung cancer-related deaths (2,3). Although significant progress has been made in the identification of the factors involved in NSCLC metastasis, the pathophysiological functions and mechanisms underlying these aberrant factors remain unclear. Estrogen receptors (ERs) are members of the nuclear steroid receptor superfamily; ERs mediate cellular responses to the hormone estrogen (4). Estradiol (E2), which is also known as 17β-estradiol, is the major and most potent product synthesized during estrogen biosynthesis, which can bind ERs and activate rapid cytoplasmic kinase signaling (5). In previous studies, we observed that activation of ERβ by estrogen in lung cancer significantly promotes tumor metastasis by increasing the expression of invasiveness-associated matrix metalloprotease 2 (MMP2) *in vitro* and *in vivo* (6). Consistent with our results, another clinical study that included over 16,000 postmenopausal female patients in the Women's Health Initiative found that higher incidence of and mortality from lung cancer occurred in women who received daily hormone replacement therapy (HRT) for over 5 years (7). However, a recent randomized phase II study, which examined the approach of coupling anti-estrogen drugs with traditional target tyrosine kinase inhibitor (TKI) therapy, found no significant differences from the results obtained using TKI therapy alone (8). Therefore, understanding the factors contributing to cancer metastasis is beneficial for the development of effective therapeutic strategies. In this study, we focused on revealing

the unknown mechanisms and key signaling pathways that promote E2-induced metastasis in NSCLC.

Toll-like receptors (TLRs) are a highly conserved family of transmembrane pattern recognition receptors that bind pathogen-associated molecular patterns (9). TLRs play a crucial role in inflammation and innate host defense against invading microorganisms by recognizing conserved motifs of microbial origin (9,10). TLR4 is specifically activated by lipopolysaccharide (LPS) from gram-negative bacterial cell walls (11). Activation of TLR4 on the respiratory epithelium activates myeloid differentiation primary response 88 (myd88) adaptor protein-dependent signaling; this phosphorylates and activates downstream signaling pathways, leading to host defense responses, including the production of inflammatory cytokines (12,13). TLR4 signaling plays an important role in maintaining tissue homeostasis, a process that is deregulated in cancer. Recent studies have shown that TLR4 activation activates mitogen-activated protein kinases (MAPKs), such as P38MAPK, ERK1/2, and JNK, leading to augmented NSCLC cell adhesion, migration, and metastasis *in vitro* and in murine NSCLC-metastasis models (14). Correspondingly, the knockdown of TLR4 can significantly suppress constitutive phosphorylation of AKT and PI3K, thereby contributing to the inhibition of human NSCLC cancer cell growth and inflammatory cytokine secretion *in vitro* and *in vivo* (15). In this process, the phosphorylation of P65 nuclear factor (NF)-κB and upregulation of MMP2 play crucial roles in promoting tumor metastasis induced by TLR4 activation (16,17); this interaction has also been recognized as the TLR4/myd88/NF-κB/MMP2 axis in signaling pathways that contribute to cancer metastasis. *In vivo*, LPS, which is specifically recognized by TLR4, increases the growth of experimental metastases in murine tumor models. How exposure to LPS affects key determinants of MMP2 overexpression has been examined previously (16).

Activated ERβ and TLR4 may similarly enhance the invasiveness of NSCLC tumor cells. MMP2, whose expression is upregulated by treatment with estradiol, can also be overexpressed by exposure to LPS. When TLR4 activates downstream signaling pathways involving P38MAPK or ERK1/2-AKT, it also triggers the activation of ERβ in the cytoplasm of NSCLC cells (4). In the present study, we used NSCLC cell lines A549 and H1793 to examine the role of ERβ in the activation of TLR4/myd88 signaling and in tumor progression and metastasis. We also used an NSCLC model to explore the tumor-promoting effect of the combined administration of estradiol and LPS *in vitro* and *in vivo*. Our results will help determine how estrogen contributes to NSCLC metastasis, which may lead to new therapies against advanced NSCLC.

Materials and methods

Clinical samples, clinicopathological analysis, and tissue microarray (TMA). This study was approved by the Institutional Ethics Committee of Tongji Medical College, Huazhong University of Science and Technology (IRB ID no. 20141101). Paired samples of primary NSCLC tumors and corresponding non-tumorous lung tissues from 241 Chinese patients were obtained at the time of surgical resection at the Department of Thoracic Surgery, Affiliated Tongji Hospital of Huazhong University of Science and Technology Tongji Medical College (Wuhan, China) from August 2013 to September 2015. None of the patients underwent chemotherapy or radiotherapy before surgery. Patient demographics, including gender, age, smoking history, pathological diagnosis, pathological tumor-node-metastasis stage (18), and tumor differentiation grade, were obtained from the Tongji Hospital records. Baseline characteristics of the patients are documented in Table I.

Among the 241 patients, metastatic lymph nodes were obtained from 30 patients with paired primary tumors; metastatic lymph nodes were obtained via surgical resection of the primary tumor with lymph node dissection. Patients with lymphadenitis and primary malignancies of the lymph node were excluded. Details on the 30 cases with IIA-IIIB NSCLC with lymph node metastasis have been provided in a previous study from our group (6). Palliative care or surgical biopsy was administered, after obtaining informed consent, to 32 patients with inoperable stage IIIb–IV primary NSCLC.

Fresh tissues were immediately snap-frozen and stored at -80˚C, or formalin-fixed and embedded in paraffin. Samples were diagnosed and confirmed by at least two lung cancer pathologists. TMA was prepared by Outdo Biotech Co., Ltd. (Shanghai, China). All patients had provided their written, informed consent to tissue collection prior to sampling, and all procedures involving human samples were conducted in accord with the Declaration of Helsinki.

Immunohistochemical (IHC) analyses. Sample processing and immunohistochemistry were performed as previously described (6). Rabbit anti-human TLR4 polyclonal antibody (Ab) (dilution 1:100, cat. no. ab13556) and rabbit anti-human ERβ monoclonal Ab (dilution 1:100, cat. no. ab3577) were purchased from Abcam. Protein expression levels were scored independently by two pathologists. Immunoreactivity scores of cancer-tissue samples were determined based on staining intensity and area of positive staining according to the method described in Tang *et al* (19). Positive cells were scored as follows: 1, ≤20% positive cells; 2, 20-50% positive cells; 3, 50-75% positive cells; and 4, >75% positive cells. Staining intensity was evaluated as follows: 1, negative; 2, weakly positive; 3, moderately positive; and 4, strongly positive. A score of 1-16 was obtained by multiplying the staining intensity and proportion of positive cells: (-), ≤4; (+), >4 and ≤; (++), >8 and ≤ 12; and (+++), >12 and ≤16. A total score >12 was defined as high expression, and a score ≤8 was defined as low expression.

Cell lines and culture conditions. Human NSCLC cell lines PC9, A549, H1793 and H1975 were purchased from the American Type Culture Collection (ATCC, Manassas, VA, USA), grown for 2 weeks, and passaged four times before freezing aliquots for subsequent analyses. The cell lines were tested and authenticated by ATCC. The normal human bronchial epithelial (HBE) cell line was obtained from the Shanghai Cancer Institute (Shanghai, China). PC9, A549, H1975 and HBE cells were cultured in Roosevelt Park Memorial Institute Medium (RPMI)-1640 medium, and H1793 cells were cultured in Dulbecco's modified Eagle's medium (DMEM):nutrient mixture F12. All media (HyClone; GE Healthcare) were supplemented with 10% fetal bovine serum

Table I. Correlation of ERβ and TLR4 expression with clinicopathological features in 241 cases of non-small cell lung carcinoma.

Patient characteristics	No. of patients (%)	ERβ expression		χ^2	P-value	TLR4 expression		χ^2	P-value
		High	Low			High	Low		
Total patient no.	241								
Sex				0.571	0.450			0.02	0.886
Female	69 (28.63)	35	34			35	34		
Male	172 (71.36)	78	94			89	83		
Age (years)				1.827	0.176			0.825	0.364
<60	139 (57.26)	60	79			75	64		
≥60	102 (42.74)	53	49			49	53		
Smoking				0.892	0.345			2.083	0.149
Ex	133 (55.19)	66	67			74	59		
Never	108 (44.81)	47	61			50	58		
T stage				2.411	0.121			0.758	0.384
1a-2b	190 (78.84)	94	96			95	95		
3-4	51 (21.16)	19	32			29	22		
Lymph node metastasis				2.145	0.143			5.732	**0.017**
Yes	118 (48.96)	61	57			70	48		
No	123 (51.04)	52	71			54	69		
Metastasis				1.000	0.585			0.765	0.471
Yes	11 (4.57)	5	6			5	6		
No	230 (95.43)	108	122			118	112		
TNM stage				0.003	0.958			3.180	0.075
I-II	151 (62.66)	71	80			71	80		
III-IV	90 (37.34)	42	48			53	37		
Tumor histology				0.141	0.707			10.152	**0.001**
SCC	84 (34.85)	38	46			55	29		
ADC	157 (65.14)	75	82			69	88		
Tumor differentiation				0.025	0.873			0.552	0.457
Well/Moderate	193 (80.09)	90	103			97	96		
Poor	48 (19.91)	23	25			27	21		

ERβ, estrogen receptor β; TLR4, Toll-like receptor 4; SCC, squamous cell carcinoma; ADC, adenocarcinoma. P-values in bold print indicate significant correlation.

(FBS; Clark Bioscience). Cells were incubated in a humidified atmosphere with 5% CO_2 and 95% air at 37˚C.

Cell transfection. The expression vectors and small interfering RNAs (siRNAs) targeting ERβ were constructed as previously described (6,20). Briefly, TLR4- or ERβ-expressing plasmids (pcDNA3.1-TLR4 or -ERβ) and corresponding empty plasmids were obtained from OriGene Technologies, Inc. siRNAs targeting TLR4 or ERβ (TLR4-siRNA or ERβ-siRNA Stealth siRNAs HSS103378; Life Technologies) and control siRNAs (ctrl-siRNA or siRNA-NC; Life Technologies) were constructed using a gene silencing vector. Lipofectamine 3000 (Invitrogen; Thermo Fisher Scientific, Inc.) was used during transfection following the manufacturer's instructions. TLR4 and ERβ protein expression was analyzed by western blotting following transfection with plasmids or siRNAs.

Drug exposure. Parental NSCLC cells and mice in the metastatic model were exposed to E2 (Sigma-Aldrich; Merck KGaA), 4,40,400-(4-propyl-[1H]-pyrazole-l,3,5-triyl), LPS (isolated from Escherichia coli 0111:B4; Sigma-Aldrich; Merck KGaA), fulvestrant (Ful; an ER antagonist; Cayman Chemical), and TAK-242 (also known as CLI-095; InvivoGen), either alone or in combination. The dosages of each drug, used *in vitro* and *in vivo*, were used as previously (21-24). Each group of cells was treated for 48 h and harvested for further analysis. Cell culture experiments were performed using reagents dissolved in 100% dimethyl sulfoxide (DMSO), and DMSO was also used as a control (vehicle).

Western blot analysis. Western blotting was performed as previously described (6). The primary antibody (Ab) used for western blots included rabbit anti-human ERβ (dilution

1:1,000) from Abcam (cat. no. ab3577), rabbit anti-human TLR4 (dilution 1:1,000) from Abcam (cat. no. ab13556), mouse anti-human MMP-2 (dilution 1:500) from Santa Cruz Biotechnology (cat. no. sc-53630), rabbit anti-human P38MAPK (dilution 1:500, cat. no. AP0424)/p-P38MAPK (dilution 1:500, cat. no. BS4844), and rabbit anti-human tAkt (dilution 1:500, cat. no. AP0485)/p-Akt (dilution 1:500, cat. no. AP0484) from Bioworld Technology, rabbit anti-human P65NF-κB (dilution 1:1,000, cat. no. ab16502)/p-P65NF-κB (dilution 1:1,000, cat. no. ab86299) from Abcam, rabbit anti-human myd88 (dilution 1:1,000) from Proteintech (cat. no. 23230-1-AP, and mouse anti-human GAPDH (dilution 1:10,000) from Cell Signaling Technology (cat. no. 51332). The densitometry of the western blots was analyzed by ImageLab software (version 6.0.0; Bio-Rad Laboratories, Inc.).

Co-immunoprecipitation. Cultured A549 cells were placed into 10-cm dishes and transfected with empty vector pcDNA3.1-ERβ, pcDNA3.1-TLR4, siRNA-ERβ, or siRNA-TLR4. The cells were then washed in 1X phosphate-buffered saline (PBS) and resuspended in 1 ml of NP-40 lysis buffer (70 mM NaCl, 50 mM Tris pH 8, and 0.5% NP-40) supplemented with phosphatase inhibitor and protease inhibitor cocktails (Sigma-Aldrich; Merck KGaA), and the cell lysates were ultrasonicated. After rotating at 4°C for 30 min, the cell lysates were collected and precleared by centrifugation at 12,000 rpm (12,800 g rcf) at 4˚C for 10 min. Protein concentration was assessed using 1 mg of total protein via the Bradford Assay (Bio-Rad Laboratories, Inc.). For co-immunoprecipitation of endogenous ERβ with TLR4, total protein was isolated from A549 cells as described previously (22). For each pull-down, 5 μg of anti-ERβ Ab (dilution 1:200, cat. no. ab3577; Abcam) or anti-TLR4 Ab (dilution 1:200, cat. no. ab30667; Abcam) was added to the normalized lysate, and the mixture was incubated overnight at 4˚C. Normal rabbit IgG (Santa Cruz Biotechnology) was used as the negative control. Immune complexes were then precipitated with protein A/G plus agarose (Thermo Fisher Scientific, Inc.). Immunoprecipitates were collected by centrifugation (2,850 x g rcf, 4˚C, 3 min) and washed gently with lysis buffer. Immunoprecipitated samples were resolved by sodium dodecyl sulfate-polyacrylamide gel electrophoresis (SDS/PAGE) for immunoblotting.

Wound-healing assay. NSCLC cell lines A549 and H1973 were cultured in a 6-well culture plate until 90% confluence. The cell monolayers were then scratched using a 200 μl sterile pipette tip. Cell migration was determined by measuring the movement of cells into the scratched area. Representative images (x40) of wound closure were captured at 0 and 24 h using an inverted light microscope (Olympus Corp.).

Cell migration and invasion assays. Transwell® Permeable Supports (inserts 6.5 mm in diameter; Corning, Inc.) were used for the cell migration assay. For the cell invasion assay, Transwell® Permeable Support inserts were coated with BD Matrigel™ Basement Membrane Matrix (BD Biosciences). Cells (A549 and H1793) suspended in serum-free media were added to the upper chamber at various densities depending on the cell line. Migration and invasion were evaluated based on the number of cells invading the Transwell® membrane, and counting was performed using an Olympus microscope (Olympus Corp.) at x100 magnification. Four fields were randomly selected for analysis. Detailed procedures are described elsewhere.

Immunofluorescence analysis. After 48 h of treatment with specific drugs or combinations of drugs, A549 and H1793 cells were seeded overnight on coverslips in a 24-well plate. After the cells reached 50% confluence, they were washed in 1X PBS, fixed with 4% paraformaldehyde for 20 min, permeabilized with 0.1% Triton X-100 for 15 min, blocked in 5% goat serum at room temperature (RT) for 30 min, and incubated overnight at 4°C with the indicated primary Ab. Next, cell-seeded coverslips were rewarmed for 1 h and incubated with a specific secondary Ab for 2 h at 37°C. Nuclei were stained with 4',6-diamidino-2-phenylindole (DAPI) for 5 min at RT. Next, the samples were washed in 1X PBS for 5 min four times. Finally, the coverslips were observed under a fluorescence microscope (Olympus Corp.; magnification of x200).

3D spheroid invasion assay. The 3D invasion assay was described previously (25). The Cultrex® 3D Spheroid Cell Invasion Assay kit (Trevigen) was utilized in this procedure. Briefly, $1x10^5$ cells in 500 ml fresh culture media containing 2.5% Matrigel and 5 ng/ml spheroid formation extracellular matrix (ECM) were plated into 24-well plates coated with a collagen/Matrigel mixture. The spheres with protrusions were considered positive for cell invasion. Distances between the invasive cell frontier and the spheroid edge were measured on day 1, 3 and 6 using an Olympus IX70 (Olympus) inverted microscope (magnification of x100). Each experiment was repeated twice, and each procedure was performed in triplicate.

Fluorescent gelatin degradation assay. Coverslips were cleaned with 20% nitric acid and coated with poly-L-lysine in a 24-well plate. Poly-L-lysine was fixed with 0.5% glutaraldehyde before adding fluorescein isosthiocynanate-conjugated (FITC) gelatin (QCM™ Gelatin Invadopodia Assay kit (Green), EMD Millipore). A thin layer of FITC-conjugated gelatin was placed onto the coverslips and was crosslinked using glutaraldehyde on ice for 10 min. Crosslinking was continued at RT for an additional 30 min. The coverslips were rinsed with PBS, incubated with 5 mg/ml sodium borohydride at RT for 3 min, rinsed again with PBS, incubated with 70% ethanol for 10 min, and dried at 37˚C for 15 min in a CO_2 incubator. One hour before plating the cells, the coverslips were quenched with RPMI-1640 containing 10% FBS at 37˚C. The cells were plated on FITC-gelatin-coated coverslips and cultured in RPMI-1640 for 24 h to quantify formation of invadopodia. Images were visualized by confocal microscopy (Olympus FV1200; magnification of x200).

Gelatin zymography. After 48 h of treatment with specific drugs or combinations of drugs, the cells were washed and incubated in serum-free medium for 24 h. MMP2 activity was measured by gelatin zymography. Samples were electrophoresed using 10% SDS-PAGE containing gelatin. After electrophoresis, the gel was washed four times with washing

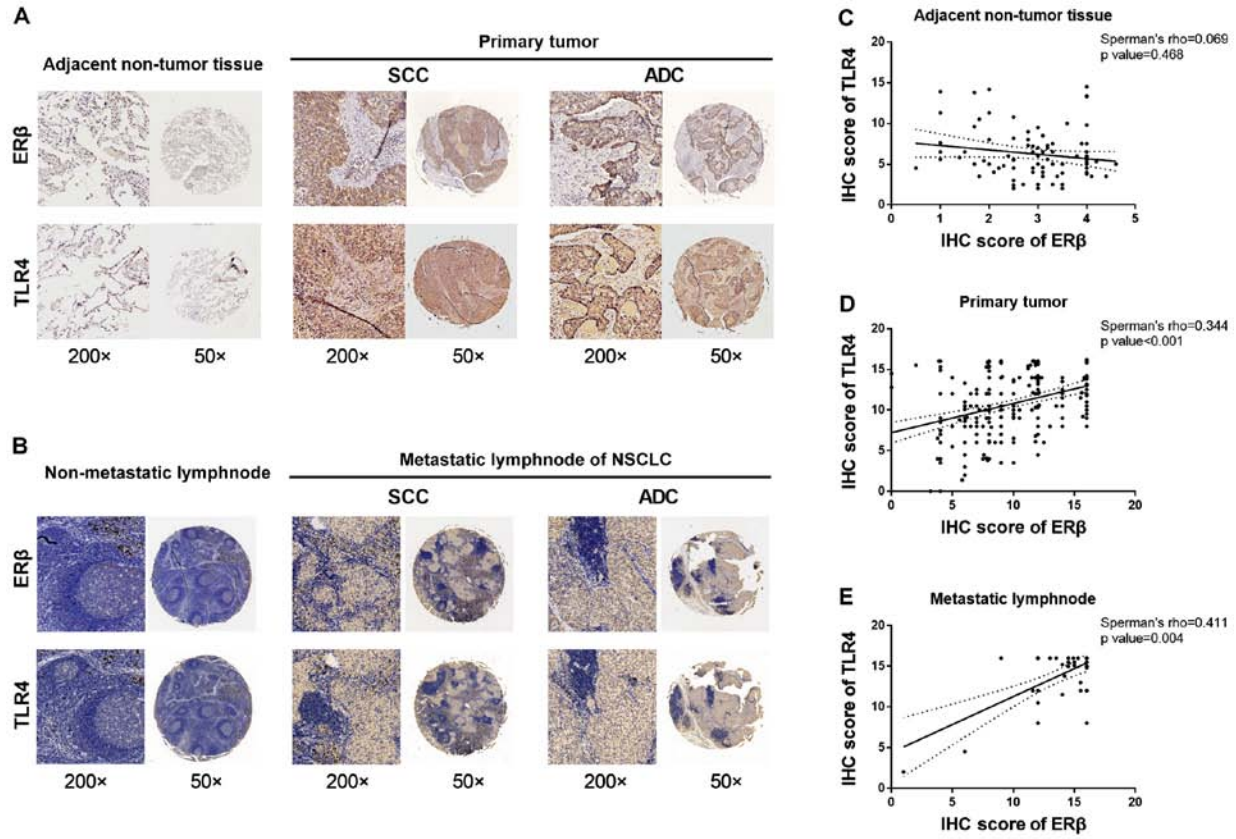

Figure 1. Expression of ERβ and TLR4 as evaluated via immunohistochemical (IHC) analyses of adjacent non-tumor tissue, primary NSCLC tissue, and metastatic lymph nodes. (A) Immunohistochemical analyses of ERβ and TLR4 expression in primary NSCLC tumor tissue and adjacent non-tumor tissue. NSCLC specimens were immunostained with ERβ and TLR4-specific antibodies. Positive cells appear as yellowish brown or contain yellowish-brown granules [magnification of x200 (left) and x50 (right)]. (B) Expression of ERβ and TLR4 in metastatic and non-metastatic lymph nodes of patients with NSCLC. (C) The correlation between ERβ and TLR4 expression in adjacent non-tumor tissue, (D) primary NSCLC tissue, and (E) metastatic lymph nodes. NSCLC, non-small cell lung cancer; ERβ, estrogen receptor β; TLR4, Toll-like receptor 4.

buffer [50 mM Tris-HCl (pH 7.5), 100 mM NaCl, and 2.5% Triton X-100], followed by a brief rinse in washing buffer without Triton X-100. The gel was incubated with incubation buffer [50 mM Tris-HCl (pH 7.5), 150 mM NaCl, 10 mM $CaCl_2$, 0.02% NaN_3, and 1 mM $ZnCl_2$] at 37˚C for 20 h. After incubation, the gel was stained by Coomassie Blue and destained. A clear zone of gelatin digestion in the gel indicated the presence of MMP2 (55 kDa).

Mouse lung metastasis model. Non-obese diabetic/severe combined immunodeficiency (NOD/SCID) female mice (4 weeks old; average weight, 15 g) were obtained from the Experimental Animal Center of Hubei Province (Animal Study Permit no. SCXK 2013-0004). The mice were maintained under specific pathogen-free conditions (System Barrier Environment no. 00127070) in the Experimental Animal Center of Tongji Hospital of Huazhong University of Science and Technology. All experiments were carried out according to the regulations specified by the Ethics Committee for Tongji Hospital of Huazhong University of Science and Technology. Mice were first intraperitoneally anesthetized with 1% sodium pentobarbital (50 mg/kg of body weight, Sigma-Aldrich, Merck KGaA) and received ovariectomy to eliminate the effects of endogenous estrogen. Next, A549 cells ($5x10^6$/100 μl) suspended in PBS were injected into the 4-week-old female NOD/SCID mice via the tail vein. Seven days after injection of the cells, the mice were randomly divided into six groups (n=5/group): mice exposed to E2 (0.09 mg/kg), mice administered E2+Ful (1.46 mg/kg), mice treated with Ful alone, mice exposed to LPS (10 mg/kg), mice exposed to a combination of E2+LPS, and negative control mice. The above-mentioned agents and combinations of agents were administered by subcutaneous injection twice per week for 10 weeks.

At week 10 after exposure, the mice were humanely euthanized by continuous inhalation with 30% CO_2 for 5 min, and were observed for 5 min to ensure the vital activity stopped. All of the experimental mice were sacrificed at the humane endpoint 10 weeks, to ensure the tumor progression time of each group was consistent. After that the lungs were surgically removed. The total number of lung nodules, lung wet weights, and lung cancer metastatic indices were statistically analyzed as previously described (6). The carcinoma tissues were then excised from the lungs; 10 mg of carcinoma tissue per mouse was homogenized in 200 ml radioimmunoprecipitation assay buffer A and subjected to western blotting.

Bioinformatics analysis. The prognostic value of ERβ/TLR4 was analyzed using the web-based Kaplan-Meier plotter (http://www.kmplot.com/lung), which is a meta-analysis tool for examining gene expression and survival data of 2,437 patients with lung cancer (2018 version) using multiple microarray data.

Table II. Correlation between ERβ expression and TLR4 in the 241 cases of NSCLC.

Tissues	Expression	$TLR4^+$	$TLR4^-$	P-value	Sperman's ϱ
Adjacent non-tumor	$ERβ^+$	19	2	0.468	0.069
	$ERβ^-$	70	22		
Primary tumor	$ERβ^+$	79	34	**<0.001**	0.344
	$ERβ^-$	45	83		
Metastatic lymph node	$ERβ^+$	22	5	**0.004**	0.411
	$ERβ^-$	10	11		

NSCLC, non-small cell lung carcinoma; ERβ, estrogen receptor β; TLR4, Toll-like receptor 4. P-values shown in bold print indicate significant correlations.

Statistical analysis. All experiments were repeated at least twice, and each procedure was performed in triplicate. All data were examined at least three times. Quantitative data are expressed as means ± SD. Statistical significance was established using the SPSS 19.0 statistical software package (SPSS, Inc.). A two-tailed P-value <0.05 was considered statistically significant.

Results

Overexpression of ERβ in NSCLC primary tumor tissues and metastatic lymph nodes correlates with TLR4 expression. Our previous research and recent studies revealed that ERβ and TLR4 are overexpressed in the cytoplasm and nuclei of NSCLC tumor tissues (15,21,22). To identify the potential roles of ERβ and TLR4 in the development and progression of NSCLC, we collected NSCLC samples from 241 patients with NSCLC and evaluated the expression of ERβ and TLR4 using immunohistochemistry. Our results showed that expression of ERβ was negative in adjacent non-tumor lung tissues, but positive in tumor tissue, and that TLR4 was highly expressed in NSCLC and normal lung tissues (Fig. 1A). Analysis of clinicopathological features indicated that high expression of TLR4 was significantly correlated with lymph node metastasis (χ^2=5.732, P=0.017) and adenocarcinoma histological type (χ^2=10.152, P=0.001; Table I). However, other clinicopathological features, including sex, age, smoking status, tumor stage, distant metastasis, and pathological tumor-node-metastasis stage, were not directly associated with the expression of ERβ or TLR4 (Table I).

We next used immunostaining to examine the association between expression of ERβ and that of TLR4 in adjacent non-tumor tissues, and in primary NSCLC tissues and metastatic lymph nodes. The results showed the correlation between ERβ and TLR4 co-expression has an increasing Spearman's rank correlation coefficient (Spearman's ϱ for short), which showed a significant positive correlation with cancer metastasis stage (adjacent non-tumor lymph nodes, primary tumor, and metastatic lymph nodes). These results are shown in Fig. 1B. The percentage of ERβ-positive stained cells was highly correlated with the level of TLR4 overexpression in metastatic lymph nodes (Spearman's correlation coefficient, r_s=0.411, P=0.004; Table II and Fig. 1E). However, no significant correlation was observed between the expression levels of ERβ and TLR4 in non-tumor lung tissue (r_s=0.069, P=0.468; Table II and Fig. 1C). A slightly stronger correlation between the expression levels of ERβ and TLR4 was observed in primary tumor tissue (r_s=0.344, P<0.001; Table II and Fig 1D). Detailed IHC scores for ERβ and TLR4 expression in primary NSCLC tumors and metastatic lymph nodes and in adjacent non-tumor tissue are shown in Fig. S1A and Table SI. Altogether, these data indicate a positive correlation between protein expression levels of ERβ and TLR4 in clinical NSCLC tissues.

Estrogen significantly upregulates the expression of TLR4 and that of the downstream myd88/NF-κB/MMP2 axis via ERβ signaling in NSCLC cell lines. LPS is a significant component of the outer membranes of gram-negative bacteria; LPS triggers TLR4 signaling (13,26). However, it remains unclear whether and how estrogen activates the signaling of ER, TLR4, and its downstream myd88/NF-κB/MMP2 axis. To evaluate the influence of estrogen on the progression of NSCLC, we first exposed NSCLC cell lines to a gradient dose (at 0, 0.1, 1, 10, 100 and 1,000 nM) and then compared the results with those of another group treated with 100 mM E2 at successive time intervals of 0, 1, 6, 12, 24 and 48 h. The results showed that TLR4 was markedly increased after E2 treatment in a dose- and time-dependent manner (Fig. 2A and B; Fig. S2A and B), and ERβ and invasiveness-associated MMP2 were also increased. We then investigated the effects of different treatments on A549 cells by administering DMSO (vehicle/negative control), E2, E2+Ful, or Ful. Our results indicated that the expression levels of TLR4 and MMP2 were significantly increased in the E2-treated group, reduced after treatment with E2+Ful, and reduced after treatment with Ful alone (P<0.05) (Fig. 2D and Fig. S2D). The baseline expression status of ERβ, MMP2, and TLR4 in different cell lines is shown in Fig. 2C and Fig. S2C. As shown in Fig. 2D and Fig. S2D, western blotting analysis further demonstrated an increase in the protein expression of myd88 and phosphorylated p-p65NF-κB, while the total levels of p65NF-κB remained unchanged in the A549 cells. To support these findings, we evaluated the expression of ERβ and TLR4 in A549 and H1793 cells using immunofluorescence analysis. TLR4 overexpression was associated with ERβ activation following

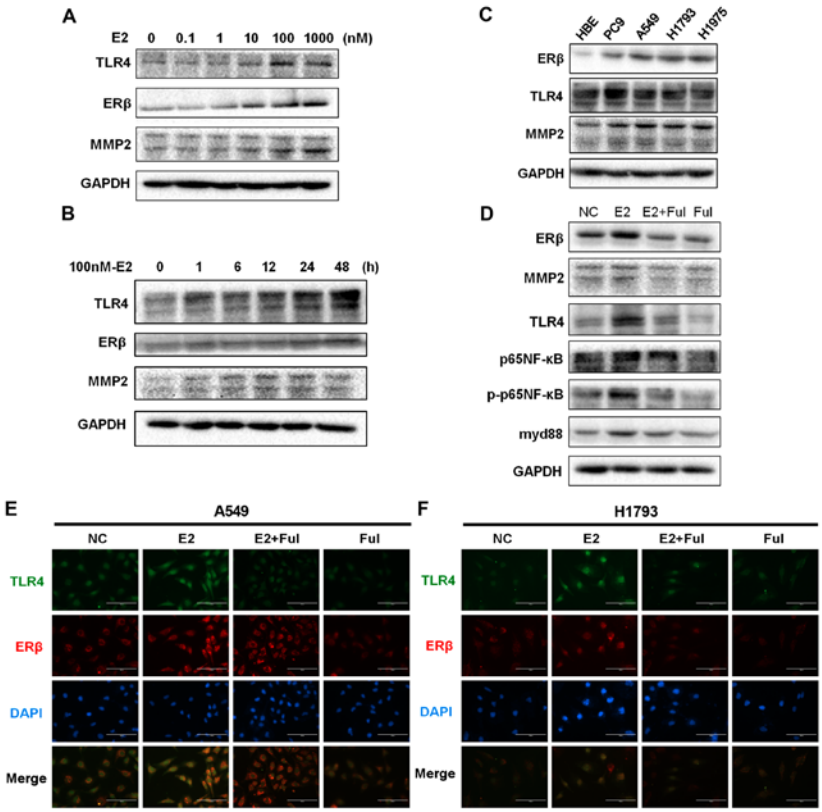

Figure 2. Protein expression of ERβ, TLR4, and the downstream myd88/NF-κB/MMP2 axis in NSCLC cell lines treated with estrogen and estrogen inhibitors. (A) The synchronized cells were exposed to E2 at different concentrations (0, 0.1, 1, 10, 100 and 1,000 nM) for 48 h. Protein expression of ERβ, TLR4, and MMP2 was analyzed using western blot analysis. The data represent mean ± SEM from three different experiments. E2 stimulated ERβ, TLR4 and MMP2 response in the A549 cell line in a dose-dependent manner. (B) The synchronized cells were treated with E2 at different time points (0, 1, 6, 12, 24 and 48 h) at concentrations of 100 nM. The data represent means ± SEM from three different experiments. E2 stimulated ERβ, TLR4, and MMP2 response in a time-dependent manner in the A549 cells. GAPDH expression was used as a control. (C) Western blot analysis of ERβ, TLR4 and MMP2 expression in cultured NSCLC cell lines (PC9, A549, H1793 and H1975) and normal bronchial epithelial cell line (HBE). (D) Western blot analysis of ERβ, TLR4, MMP2, p65NF-κB, phosphorylated (p)-p65NF-κB, and myd88 protein levels at 48 h in A549 cells. Estrogen exposure significantly upregulated the expression of TLR4 and activated the myd88/NF-κB/MMP2 pathway, while anti-estrogen drugs showed the opposite effect. GAPDH expression was used as a control. (E and F) Immunofluorescence staining of ERβ and TLR4 in A549 and H1793 cells. Scale bar, 200 μm. NSCLC, non-small cell lung cancer; MMP2, matrix metalloprotease 2; ERβ, estrogen receptor β; TLR4, Toll-like receptor 4; myd88, myeloid differentiation primary response 88; NF-κB, nuclear factor-κB.

exposure to E2 (Fig. 2E and F). Expression of TLR4 and the activation of its signaling pathways were markedly affected by E2. These results indicate a positive correlation between the expression of ERβ and that of TLR4 during NSCLC metastasis.

Inhibition of ERβ expression by siRNA decreases TLR4 expression. To investigate how ERβ expression affects the expression of TLR4, ERβ-targeting siRNA or NC siRNA was transfected into NSCLC A549 and H1793 cells to generate a specific ERβ-knockdown cell model. In contrast, an ERβ-overexpression cell model was generated by transfecting an ERβ expressing pcDNA-plasmid into the A549 and H1793 cells. The changes in ERβ and TLR4 expression were evaluated by western blot and immunofluorescence analyses (Fig. 3A and B; Fig. S3A). Our results revealed that removal of endogenous ERβ expression significantly suppressed the expression of TLR4, while overexpression of ERβ significantly promoted the expression of TLR4. In addition, inhibition of ERβ expression significantly decreased expression of MMP2 and myd88. These results indicate that the expression levels of ERβ and TLR4 were positively associated with NSCLC progression.

Suppression of downstream signaling pathways impairs the effect of TLR4 upregulation induced by treatment with estrogen. After treatment with estrogen, cytoplasmic kinase signaling is rapidly activated via ERβ signaling in seconds to minutes. This rapid signaling is termed non-genomic and occurs via non-nuclear ERs located in the membrane or cytoplasm of the cell (27). Our previous research showed that MMP2 upregulation is affected by ERK/P38MAPK and PI3K/AKT signaling pathways activated by estrogen (6). Therefore, we next investigated how the expression of ERβ affects that of TLR4 and downstream signaling pathways. For this, several inhibitors were used to determine the effect of estrogen during blockade of the expression of TLR4/myd88, ERK/P38MAPK, or PI3K/AKT. TAK-242 is a selective inhibitor that suppresses the interaction between TLR4 and its adaptor molecules; this suppression occurs via the intracellular Cys747 residue of TLR4 (23,28). Our results showed that the upregulated expression of TLR4 and MMP2 induced by treatment with estrogen was reversed by treatment with TAK-242 (Figs. 3F and S3E) or with TLR4 siRNA (Figs. 3G and S3F). Next, to support these findings, we performed Transwell migration/invasion assays. Our results demonstrated that invasiveness and aggressiveness of the cells, induced by treatment with E2, were impaired by

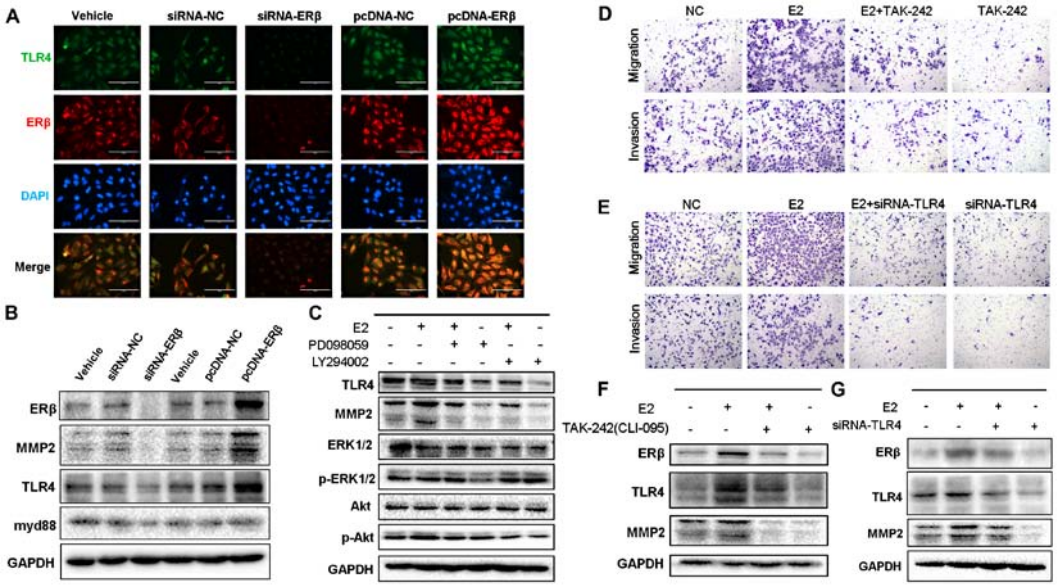

Figure 3. Protein expression of ERβ and TLR4 under RNAi intervention or overexpression of ERβ. (A) Immunofluorescence staining of ERβ and TLR4 in siRNA-ERβ- and pcDNA-ERβ-treated A549 cells. Scale bar, 200 μm. (B) Decreased protein levels of TLR4, MMP2, and myd88 in siRNA-ERβ-treated A549 cells compared with those in siRNA-NC-treated cells as evaluated by western blotting. The panel also showed increased expression of TLR4, MMP2, and myd88 in cells treated with pcDNA-ERβ. (C) Western blot analysis of TLR4, MMP-2, p-p38MAPK, P38MAPK, pAKT, and AKT protein levels in A549 cells treated with E2, PD098059, or LY294002, in combination or alone. The upregulation of TLR4 signaling pathway by E2 was inhibited when either ERK/MAPK or PI3K/AKT was blocked. GAPDH expression was used as a control. (D) Representative images of Transwell assays used to assess E2-induced NSCLC cell invasiveness and migration with or without treatment with TAK-242, a specific antagonist of TLR4. TLR4 blocked by TAK-242 impaired the invasiveness of NSCLC cells treated with E2. (E) Representative images of Transwell assays used to assess E2-induced NSCLC cell invasion and migration with or without siRNA-TLR4 interference. TLR4 knockdown by siRNA impaired the invasiveness of A549 cells treated with E2. (F) Representative blot showing decreased protein expression of MMP2 when TLR4 expression was blocked by TAK-242. (G) Representative blot showing decreased protein expression of MMP2 in TLR4 knockdown cells induced by siRNA. NSCLC, non-small cell lung cancer; MMP2, matrix metalloprotease 2; ERβ, estrogen receptor β; TLR4, Toll-like receptor 4.

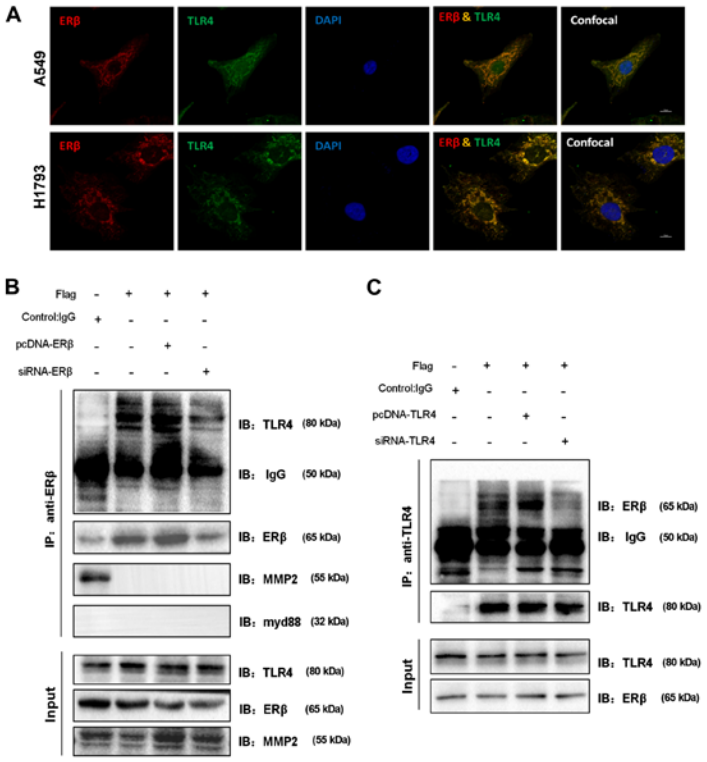

Figure 4. ERβ co-localizes and interacts with TLR4 in NSCLC cell lines. (A) Representative confocal images of cells treated with E2 (100 nM, 48 h) showing co-localization (in yellow) of endogenous ERβ with TLR4 in A549 and H1793 cells. Scale bar, 10 μm. (B) ERβ co-immunoprecipitates with endogenous TLR4 but not with myd88 or MMP2. Cell lysates were prepared from A549 cells and immunoprecipitated (IP) with rabbit ERβ or control IgG antibodies. Precipitates were resolved by 10% SDS-PAGE, followed by immunoblotting (IB) with rabbit TLR4, rabbit myd88, and rabbit MMP2. Protein levels of TLR4, MMP2, and ERβ in 1% of total input cell lysate are also shown. (C) TLR4 co-immunoprecipitates with endogenous ERβ as assessed by co-immunoprecipitation analysis. NSCLC, non-small cell lung cancer; MMP2, matrix metalloprotease 2; ERβ, estrogen receptor β; TLR4, Toll-like receptor 4; myd88, myeloid differentiation primary response 88.

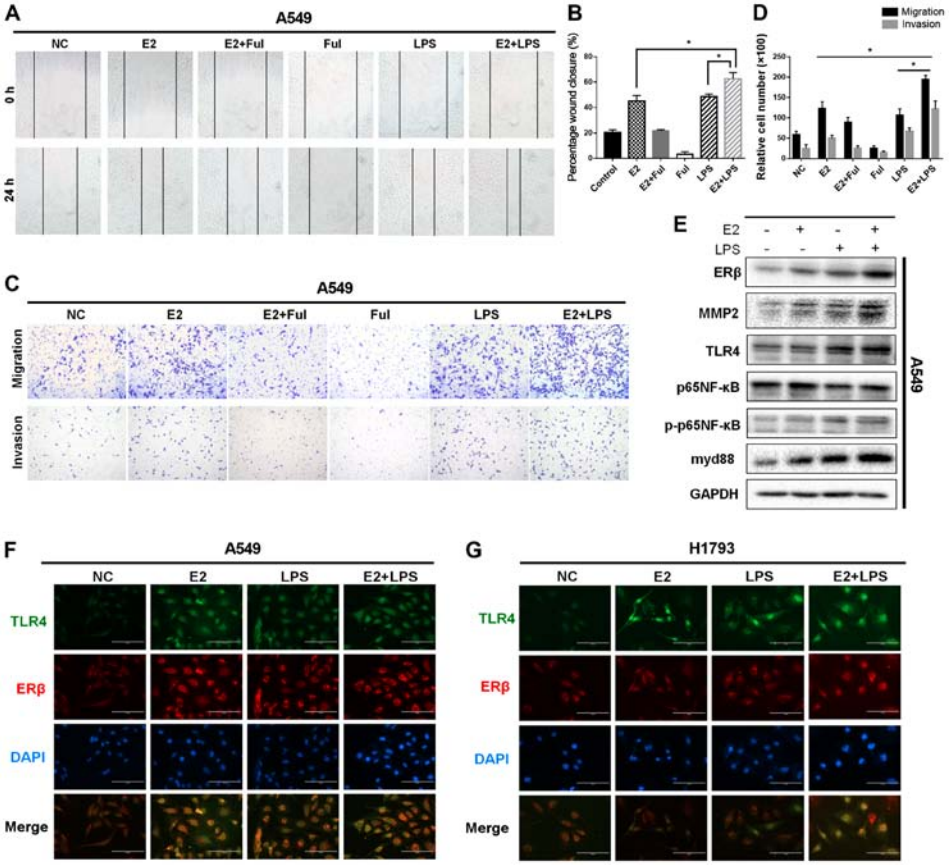

Figure 5. Activation of ERβ and TLR4 synergistically promotes migratory/invasive abilities of NSCLC cells. (A) Migration in a wound-healing assay of A549 cells after treatment with DMSO (negative control, NC) or E2 (10 nM), Ful (1 μM), E2+Ful, LPS (10 μg/ml), and E2+LPS for 24 h (magnification x40). (B) Effect on wound closure (shown as a percentage) in A549 cells. (C and D) Matrigel Transwell assays were performed to determine the invasiveness of A549 cells in different treatment groups. Treatment with E2 and LPS enhanced cell invasion, while the combination of E2 and LPS increased cell invasiveness more than did treatment with either agent alone. (E) Western blot analysis of ERβ, TLR4, MMP2, p65NF-κB, phosphorylated (p)-p65NF-κB, and myd88 protein levels at 48 h in A549 cells, respectively. Protein levels of ERβ, TLR4, myd88, MMP2, and phosphorylation of P65NF-κB, induced by the combined treatment of E2 and LPS, were much higher compared with those in cells treated with E2 or LPS alone. (F and G) Immunofluorescence staining of ERβ and TLR4 expression in A549 and H1793 cells. Scale bar, 200 μm. *P<0.05 indicates statistical significance. NSCLC, non-small cell lung cancer; LPS, lipopolysaccharide; Ful, fulvestrant (ER antagonist); MMP2, matrix metalloprotease 2; ERβ, estrogen receptor β; TLR4, Toll-like receptor 4; myd88, myeloid differentiation primary response 88; NF-κB, nuclear factor-κB.

blocking (Figs. 3D and S3C) or silencing (Figs. 3E and S3D) TLR4 signaling. We then used the pAkt inhibitor LY294002 and the pERK inhibitor PD098059 to treat A549 cells and found that TLR4 expression was significantly abrogated when expression of ERK/P38MAPK and PI3K/AKT was suppressed (P<0.05); this effect was sustained even after exposure to E2 (Figs. 3C and S3B). Altogether, these findings confirm that promotion of NSCLC cell metastasis induced by E2 may be reversed by inhibiting the signaling of TLR4. Our results also showed that activation of the ERK/P38MAPK and PI3K/AKT pathways was required for ERβ-mediated TLR4 upregulation and was necessary to enhance migration and invasiveness of NSCLC cells.

ERβ co-localizes with TLR4 in the NSCLC cell lines. We next used immunofluorescence analysis to evaluate the potential molecular mechanisms underlying the positive association between the expression of ERβ and that of TLR4. For this, A549 cells were treated with 100 nM E2 for 48 h. Indirect immunofluorescence analysis indicated that endogenous expression of ERβ and TLR4 was primarily co-localized in the cytoplasm, while the nuclear region showed sparse co-expression (Fig. 4A). Similar results were observed in the cytoplasm of another NSCLC cell line, H1793. In this cell line, co-localization was particularly visible under higher magnification and at a higher resolution. These data indicate that ERβ and TLR4 proteins likely form a complex or interact with each other.

Novel ERβ-TLR4 interaction. Previous studies have shown that the amino-terminal region of ER enables it to dimerize or bind to co-activators, co-repressors, regulators, and ligands. This binding is responsible for the promotion of enhanced tumorigenesis (27,29). Our previous findings indicated a positive signaling association and interaction between ERβ and TLR4. This prompted us to examine whether there are direct physical and molecular interactions between ERβ and TLR4. To determine whether endogenous ERβ and TLR4 interact with each other, we co-immunoprecipitated ERβ with TLR4 using cell lysates isolated from A549 cells. TLR4 was readily detected in ERβ immunoprecipitates (Fig. 4B), while ERβ was found in TLR4 immunoprecipitates (Fig. 4C). However, the interaction of endogenous myd88 or MMP2 with ERβ was not detected (Fig. 4B). Hence, our results indicate that there is an interaction between ERβ and TLR4. These data suggest

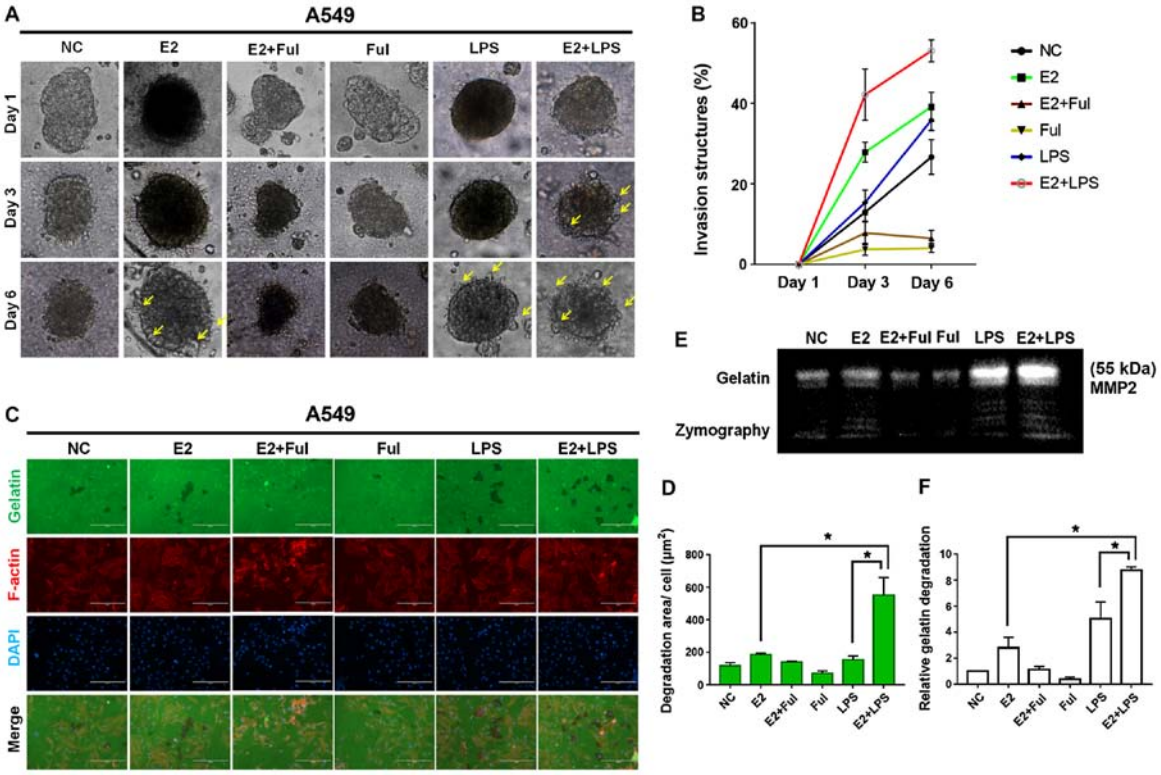

Figure 6. Combined treatment with estrogen (E2) and LPS accelerates invadopodium formation in NSCLC A549 cells. (A) 3D spheroid cell invasion assay of lung adenocarcinoma A549 cells treated with DMSO (negative control, NC), E2 (10 nM), Ful (1 μM), E2+Ful, LPS (10 μg/ml), and E2+LPS. Representative images were acquired on day 1, 3 and 6 via light microscopy (x100). Combined treatment of E2+LPS accelerated invadopodium formation (yellow arrow) compared with other treatments. (B) Quantification of 3D spheroid cell invasion assays. Quantification was carried out by measuring the distance between the invasive cell frontier and the spheroid edge. (C) To confirm the invasive activity of cancer cells, slides were coated with FITC-conjugated gelatin (green). NSCLC cells were cultured on the FITC-gelatin-coated coverslips for 36 h. To visualize F-actin, phalloidin (red) and DAPI (blue) were used to stain cytoplasm and nuclei, respectively. Punctuate black areas indicate representative degraded gelatin regions. Scale bar, 200 μm. (D) Quantification of degradation level in FITC-gelatin as assessed by degradation assay (area per cell, μm^2). (E and F) The activity of MMP2 was assessed by gelatin zymography. The aggressiveness of NSCLC cells was higher in the E2+LPS-treated group than in the other treatment groups. *P<0.05 indicates statistical significance. NSCLC, non-small cell lung cancer; LPS, lipopolysaccharide; Ful, fulvestrant (ER antagonist); MMP2, matrix metalloprotease 2.

that the interaction of ERβ and TLR4 in cellular cytoplasm contributes to NSCLC metastasis.

Activation of ERβ and TLR4 expression synergistically promotes migratory and invasive abilities of the NSCLC cells. After confirming that exposure to E2 induced endogenous interaction of ERβ and TLR4 and increased TLR4 protein levels, we assessed the extent to which the metastatic aggressiveness of the human NSCLC A549 and H1793 cell lines was mediated by exposure to E2, LPS, and combined administration of E2+LPS. The wound-healing assay revealed that cells treated with E2+LPS significantly increased their rate of lateral migration into wounds introduced on confluent cellular monolayer, compared with the rate of lateral migration shown by the single-drug-treated groups and inhibitor-treated groups (A549 cells: Fig. 5A and B, P<0.05; H1793 cells: Fig. S4A and B, P<0.05). To detect and quantify the aggressiveness of NSCLC cells, we next performed Transwell migration\invasion assays. The highest number of invading cells was found in the E2+LPS treated group. These results indicate that treatment with E2+LPS increased the metastatic abilities of the NSCLC cells (A549 cells: Fig. 5C and D, P<0.05; H1793 cells: Fig. S4C and D, P<0.05). Western blotting and immunofluorescence staining were used to determine the expression levels of different proteins involved in the ERβ/TLR4 interaction and downstream signaling pathways (A549 cells: Figs. 5E and F and S4E; H1793 cells: Figs. 5G and S5C and D). The results of the densitometric analysis showed that the levels of ERβ, TLR4, myd88, and MMP2 proteins and phosphorylation of p65NF-κB (p-p65NF-κB) induced by the treatment with E2+LPS were significantly higher than were those induced by treatment with E2 or LPS. Taken together, our findings indicate that activation of ERβ and TLR4 synergistically promoted the metastatic abilities of the NSCLC cells.

Combination of estrogen and LPS accelerates invadopodium formation in the NSCLC cells. Increased cell invasion in metastatic progression is induced by invadopodium formation followed by extracellular matrix (ECM) degradation (30,31). Hence, we explored whether the combined exposure to E2 and LPS accelerates invadopodium formation and ECM degradation. We performed *in vitro* Matrigel 3D spheroid invasion assays using A549 and PC9 cells administered E2, LPS, E2+LPS, and DMSO (vehicle) to evaluate invasiveness in the cell lines. Density and length of cell-invasion structures were evaluated on days 1, 3 and 6. Compared with negative control treatment, exposure to E2 or LPS alone significantly increased the invasive capability of cells, which formed invadopodia on day 6. The group treated with E2+LPS showed accelerated formation of invadopodia on day 3 (A549 cells: Fig. 6A and B).

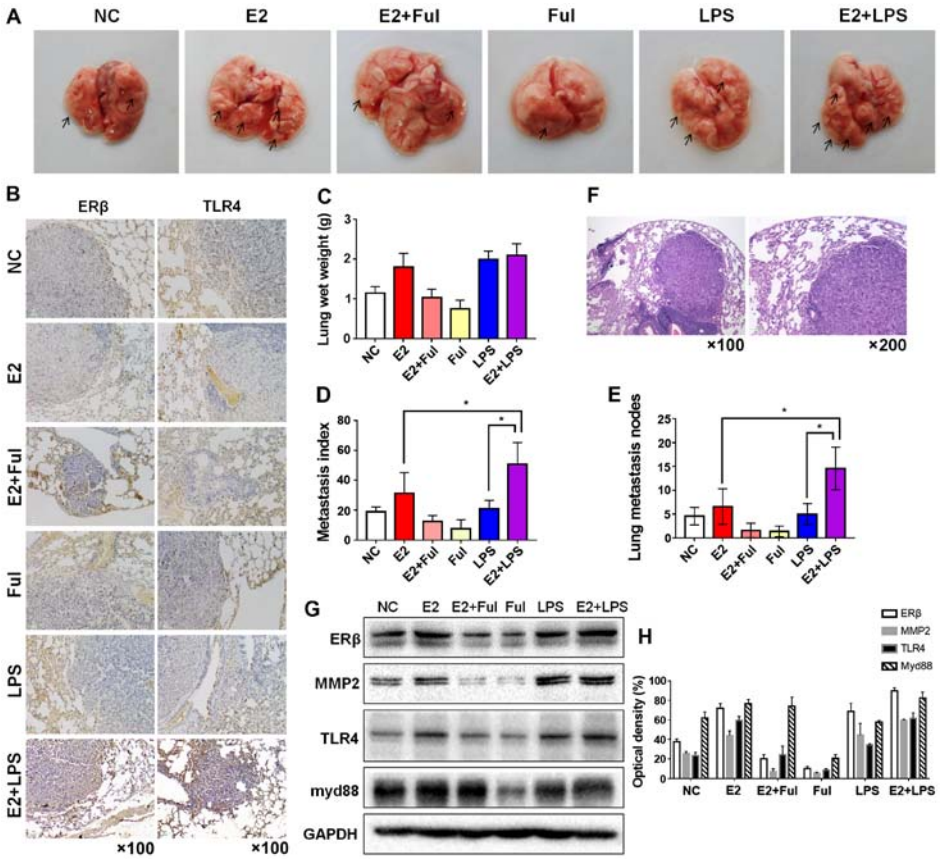

Figure 7. Combination of estrogen (E2) and LPS synergistically enhances tumorigenicity and metastatic ability in a metastatic mouse model. (A) Bilateral ovariectomy was performed in 4-week-old female NOD/SCID mice. Then, NSCLC A549 cells ($5x10^6$/100 μl) suspended in PBS were injected into the 4-week-old female NOD/SCID mice via the tail vein, and the mice were randomly divided into six groups (n=5/group) as follows: negative control, E2-treated (0.09 mg/kg), E2+Ful-treated (1.46 mg/kg), Ful+LPS treated (10 mg/kg) and E2+LPS-treated groups. The lungs were removed after 6 weeks of drug treatment. Gross appearance of metastatic lung tumor nodes in different treatment groups is indicated by arrows. (B) IHC staining of ERβ and TLR4 expression in murine lung metastatic nodes in each group (magnification x100). (C) Mean lung wet weight of each group, (D) metastatic indices in the different groups (definition mentioned in the 'Materials and methods') and (E) the number of metastatic nodules in the lungs (number of lung nodules in every mouse of each group). Mice treated with E2 and LPS showed the highest lung wet weight, highest number of lung metastatic lesions, and the highest metastasis index values, compared with mice injected with normal saline (negative control) and the other treatment groups. (F) Hematoxylin and eosin staining of murine lung metastatic nodes acquired at a magnification of x100 and x200. (G) Protein expression of ERβ, MMP2, TLR4, and myd88 in murine lung metastatic nodes was analyzed using western blot analysis and (H) analysis of optical density. *P<0.05 indicates statistical significance. NSCLC, non-small cell lung cancer; LPS, lipopolysaccharide; Ful, fulvestrant (ER antagonist); MMP2, matrix metalloprotease 2; ERβ, estrogen receptor β; TLR4, Toll-like receptor 4; myd88, myeloid differentiation primary response 88.

The H1793 cells failed to form spheroids in Matrigel media; therefore, we used PC9 NSCLC cells for this procedure (PC9 cells: Fig. S5A and B). Invadopodia appear as accumulations of F-actin associated with dark areas of fluorescent gelatin degradation (31,32). To fully determine whether the combination of E2 and LPS enhanced the function of invadopodia, we conducted a fluorescent gelatin degradation assay and gelatin zymography analysis. The co-localization of F-actin with gelatin degradation induced in cells treated with estrogen or LPS related-drugs compared with that in unstimulated cells is shown in Fig. 6C. A549 cells treated with E2+LPS showed over 400 μm^2 dark degradation area/cell, while single-drug-treated groups of cells showed barely 200 μm^2 degraded area/cell (Fig. 6C and D), and we repeated this procedure with H1793 cells (Fig. S6A and B). Consistently, the results of gelatin zymography also showed that exposure to E2+LPS induced more ECM degradation in the cells than did exposure to the single agents (Fig. 6E and F). Together, these data indicate that the combination of estrogen and LPS strongly accelerated and enhanced invadopodia function in NSCLC cells.

Combination of estrogen and LPS synergistically enhances the tumorigenicity and metastatic ability in a metastatic mouse model. The effect of combined exposure to E2 and LPS in cancer metastasis, which was demonstrated *in vitro*, was further confirmed in an animal model. For this, female ovariectomized NOD/SCID mice were injected with A549 cells into the tail vein. After 65 days of treatment, mice from each group (n=5) were sacrificed, and the number of metastatic nodules in the lungs was examined at the indicated time points. As expected, mice exposed to the combination of E2 and LPS showed higher lung wet weights, numbers of lung metastasis lesions, and metastatic indices than did mice injected with normal saline (negative control) or other treatments (Fig. 7A, and C-E). Hematoxylin and eosin staining for metastatic nodules is shown in Fig. 7F. We then used western blotting and immunohistochemistry to assess protein levels in each group of mice. As shown in Fig. 7G and H, the expression of ERβ and TLR4 in the E2+LPS-treated group was significantly higher than that in groups exposed to either of E2 or LPS alone, and expression levels were decreased in

the E2+Ful- and Ful-treated groups. Consistently, invasiveness-associated overexpression of MMP2 was higher in the group treated with E2+LPS than that in the groups subjected to other treatments. Additionally, the immunohistochemical staining of ERβ and TLR4 in murine metastatic lung tissues is shown in Fig. 7B. Altogether, our findings showed that the combination of E2+LPS synergistically increased lung metastasis in the mouse tumor model.

Discussion

Metastatic dissemination and disease relapse are significant causes of poor clinical outcome in patients with non-small cell lung cancer (NSCLC). The vast majority of cancer-related deaths are due to metastasis rather than to the influence of the primary cancer (2,3). Recently, estrogen has been found to play a crucial role in promoting malignant cancers, including in target organs of breast cancer metastasis and non-target cancers (5,29). We previously revealed that estrogen promotes NSCLC tumor metastasis via estrogen receptor β (ERβ) signaling and upregulation of matrix metalloprotease 2 (MMP2) expression. However, we did not determine the exact mechanisms involved in this process (6). ERs can regulate Toll-like receptor (TLR) signaling pathways in the immune system (33), but how and whether ERβ triggers TLRs in NSCLC remains unknown. In the present study, we performed *in vitro* and *in vivo* investigations to determine the mechanisms that regulate the activity of TLR4 and how it affects the downstream myeloid differentiation primary response 88 (myd88)/nuclear factor (NF)-κB /MMP2 signaling axis. We found that treatment with estrogen and the combined activation of ERβ and TLR4 significantly enhanced cell motility, invasiveness, and extracellular matrix (ECM) degradation. Additionally, we observed increasing overexpression of ERβ and TLR4 at metastatic stages, in particular, within lymph nodes, but not in the primary site of human NSCLC tumor tissues. These considerations prompted us to further investigate estradiol (E2) and lipopolysaccharide (LPS) exposure of NSCLC *in vitro*.

TLR4 is a member of the Toll-like receptor family and was initially identified as the specific receptor for LPS (9,10). TLR4 is expressed in normal epithelial cells and immune cells and plays a physiologically relevant role in innate immunity as the first line of host defense (34). TLRs are considered significant factors implicated in chronic inflammatory-driven carcinogenesis (35). Activation of TLR4 promotes NSCLC metastasis *in vitro* and *in vivo* (14-17). Chow *et al* (14) demonstrated that enhanced adhesion and migration abilities of the NSCLC cell line A549 decreased when the expression of TLR4s, P38MAPK, and ERK1/2 was blocked with specific inhibitors; TLR4 blockade was also found to abrogate hepatic metastasis in the NSCLC murine cell line H59. Li *et al* also showed that knockdown of TLR4 markedly inhibited the growth of human NSCLC cancer cells (15). Consistently, we demonstrated increased cell migration and invasion of A549 and H1793 cells following exposure to LPS (Fig. 5). We also observed higher numbers of murine lung metastatic nodules in the LPS-exposure group of mice than in the control mice (Fig. 7). In addition, the phosphorylation of p38MAPK and pAkt was evaluated by western blotting, which is also consistent with previous reports (16,17). Altogether, these results indicate that the TLR4/myd88/NF-κB/MMP2 axis plays a crucial role in promoting NSCLC metastasis.

ERβ was previously found to significantly increase NSCLC cell invasiveness by upregulating the expression of MMP2 (6). Thus, we investigated the relationship between TLR4 and ERβ. To clarify the association between TLR4 and ERβ, we analyzed the expression levels of TLR4 and ERβ in NSCLC primary tumors, metastatic lymph nodes, and adjacent non-tumor lung tissues. Interestingly, our results showed that the association of ERβ and TLR4 promoted metastasis in a grade-dependent manner. As shown in Table II, the Spearman's rank correlation coefficient was higher for metastatic lymph nodes than for primary tumors, while no statistical difference was detected in non-tumor tissue. In a previous study from our group, we reported that patients with lung cancer express high protein levels of ERβ in metastatic lymph nodes compared with these levels in primary tumor tissues (6). In this previous investigation, we found significant levels of co-expression of ERβ and MMP2 in primary tumors, but no co-expression in lymph nodes. This raised the question of whether estrogen-induced ERβ can regulate MMP2 expression directly during metastasis. The results of our present study indicate that exposure to E2, or upregulation of ERβ, increased the expression levels of both TLR4 and MMP2 in NSCLC cells. To determine whether MMP2 overexpression was induced mainly by activation of TLR4, we used RNA interference to knock down TLR4 in A549 cells while treating the cells with E2. Our results showed that MMP2 overexpression and increased cell invasiveness induced by treatment with E2 were attenuated by the silencing of TLR4. Furthermore, ERβ was found to immunoprecipitate with TLR4, and TLR4 was found to immunoprecipitate with ERβ, demonstrating a direct physical interaction between ERβ and TLR4 proteins. The co-immunoprecipitation assay showed no direct binding of ERβ with MMP2 or myd88. The results of our confocal micrography were consistent with the above results. Still, these findings do not exclude the possibility that this interaction may require other proteins. This finding may explain why ERβ shows no correlation with MMP2 in metastatic lymph nodes, but is strongly associated with TLR4, although a significant correlation between ERβ-TLR4 and ERβ-MMP2 could be detected in primary tumor tissues. Taken together, our data indicate that activated ERβ and TLR4 interact with each other in the cell plasma, contributing to NSCLC metastasis.

Unfortunately, the results of our prognostic analysis were not included in this study due to a significant loss to follow-up (overall loss to follow-up rate = 28.63%; disease-free survival follow-up loss ratio = 38.15%). However, using the Kaplan-Meier survival analysis of expression data from 1,928 patients with NSCLC (http://www.kmplot.com/lung), we found that high co-expression of ERβ and TLR4 was significantly associated with poor overall survival, with a hazard ratio (HR) = 1.21 (log-rank test P=0.0031). These results indicate that a high co-expression of ERβ and TLR4 can predict poor survival in patients with NSCLC, and overexpression of ERβ and TLR4 may contribute to tumor development (Fig. S1B-D). Our prognostic data for this patient population will be further evaluated.

Multiple studies have shown that the effect of estrogen on the progression of lung cancer may be associated with other signaling pathways (4,5). Importantly, malignant tumor carcinogenesis progresses rapidly and dramatically when ERβ is activated and synergistically cooperates with other cancer-promoting signaling pathways. Previously, we showed a synergistic cooperation between ERβ and IGF-1 in NSCLC cells (19). In the present study, the *in vitro* analysis showed that the combined administration of E2 and LPS markedly upregulated protein expression levels of ERβ and TLR4. Furthermore, we observed the co-localization and direct bingding of ERβ and TLR4 in cell experiments. These results spurred us to investigate whether the interaction between ERβ and TLR4 synergistically enhances the metastatic aggressiveness of lung cancer cells. The results of our *in vitro* and *in vivo* analyses showed that the combined administration of E2 and LPS enhanced the mobility and invasiveness of NSCLC cells more than did exposure to each agent alone. Using a wound-healing assay, we showed that both A549 and H1793 cells treated with E2+LPS generated a significantly narrower wound closure than did those treated with E2 or LPS alone; similar responses were observed in the Transwell assay. Our results obtained using *in vivo* studies showed the highest number of metastatic lung nodules, wet lung weights, and metastasis indices in the group exposed to the combination of E2 and LPS. These results indicate that estrogen synergistically promoted the metastasis of NSCLC via the ERβ and TLR4 signaling pathways. These results also indicate that ERβ and TLR4 are two key signaling molecules involved in the synergistic activity of the two pathways mediating the progression of NSCLC.

However, in our mouse experiments, endogenous estrogen also affected the activation status of ERβ and TLR4 in the internal environment. To avoid the physiological hormone, we treated mice with a necessary large dose of estradiol/E2 (0.09 mg/kg) (19) and LPS (10 mg/kg) (24) to show the effect of promoting NSCLC metastasis. These doses are high enough to ignore the effect cause by murine endogenous hormone. On the other hand, in human tissues, it has been confirmed that primary NSCLC tissues are equipped to secret E2 (27), thus the endogenous estrogen in blood does not reflect the local hormone effect of NSCLC tissue. That was the reason why we used immunostaining to examine the association between expression of ERβ and TLR4 to analyze the tumor-promoting effect of E2 and LPS. Additionally, our cell culture experiment also confirmed the increased promoting effect of NSCLC metastasis following exposure to E2 and LPS.

During metastasis, cancer cells dissociate from a primary tumor mass by degrading the extracellular matrix (ECM) to locally invade the tumor stroma and adjacent tissues (36). Cancer cells achieve detachment, degrade the ECM, and migrate by forming unique membrane structures called invadopodia (30,31). In the present study, we demonstrated that stimulation with E2, LPS, or both E2 and LPS provided NSCLC cells with increased ability to degrade the surrounding FITC-gelatin ECM after a 24 h incubation, and accelerated the formation of invadopodia in the 3D spheroid invasion model. As expected, the analysis revealed higher aggressiveness in NSCLC cells exposed to the combination of E2 and LPS than in those exposed to either individual agent. Thus, the interaction and cooperation of ERβ and TLR4 pathways promote ECM degradation by NSCLC cells and accelerate the formation of invadopodia, thereby enhancing invasiveness. One of the most critical functions of mature invadopodia is enhancing the activity of excretive MMP2. Functional enzymes localized at the invadopodium surface membranes enable proteolytic activity and promote MMP2 activation to initiate the MMP activation cascade, which involves the conversion of proMMP2 to active MMP2 (37,38). ProMMP2 cannot efficiently degrade the ECM unless it is activated. In the present study, we observed that overexpression of the MMP2 protein was induced by combined exposure to E2+LPS. This result suggests that stimulation with estrogen may not only upregulate MMP2 but may also play a role in MMP2 activation.

Even though our study mainly focused on the protein levels of many relevant moleculars and utilized different types of experiments for analysis, there are still some limitation to our research. The genomic response of each gene of ERβ and TLR4 was not analyzed or how the interaction between these two receptors could cause the synergistic tumor metastasis-promoting effect, which both would still be another interesting research topic. The exact gene function and deeper mechanistic understanding of the upregulation of TLR4 require more investigation in our future study. In addition, the activation of another estrogen receptor G-protein-coupled estrogen receptor (GPER), may also be triggered by estrogen (39) and was confirmed to promote NSCLC proliferation in our previous study (22); however, there is still no evidence to suggest that GPER signaling is able to trigger TLR4 signaling in non-genomic pathways to date.

In summary, our study highlights the novel role and regulatory mechanisms of estrogen in promoting NSCLC metastasis via ERβ by upregulating the expression of TLR4 and activating its downstream myd88/NF-κB/MMP2 signaling axis. Importantly, in the present study, we revealed the interaction and correlation between the ERβ and TLR4 signaling pathways. Additionally, we showed the combined effect of E2 and LPS in promoting NSCLC cell invasiveness and in accelerating the formation of invadopodia. Understanding how the multiple activities of ERβ contribute to invasive phenotypes of cancer cells will be the focus of our future studies. Targeting of ERβ may provide novel strategies for treating patients with advanced metastatic lung cancer.

Acknowledgements

We all deeply thank Mrs. Huifang Liang of the Hepatic Surgery Center of Tongji Hospital for her technical assistance. The cell lines used in this study were provided by the American Type Culture Collection (ATCC).

Funding

This study was funded by the National Natural Science Foundation of China (NSFC) (grant nos. 81272590 and 81572277).

Availability of data and materials

All relevant data are included in the manuscript and in the Supplementary materials files.

Authors' contributions

SF and YL designed and conceived the study with the professional help of LL and XC. SF, WQ, QH and HX performed the experiments. CL, DL, SZ, BA, and HL carried out the technical aspects of the research and materially supported the experiments. SF and YL wrote the manuscript. The manuscript was edited and revised with the help of LL and XC. All authors read and approved the manuscript and agree to be accountable for all aspects of the research in ensuring that the accuracy or integrity of any part of the work are appropriately investigated and resolved.

Ethics approval and consent to participate

The study was approved by the Ethics or Institutional Review Board of Tongji Hospital (Wuhan, Hubei, China) (no. 20141101), and written, informed consent was obtained from all subjects in accordance with the Declaration of Helsinki. All animal experiments were carried out according to the regulations specified by the Ethics Committee for Tongji Hospital of Huazhong University of Science and Technology.

Patient consent for publication

Not applicable.

Competing interests

The authors declare that they have no competing interests.

References

1. Siegel RL, Miller KD and Jemal A: Cancer Statistics, 2017. CA Cancer J Clin 67: 7-30, 2017.
2. Langer CJ, Besse B, Gualberto A, Brambilla E and Soria JC: The evolving role of histology in the management of advanced non-small-cell lung cancer. J Clin Oncol 28: 5311-5320, 2010.
3. Ferlay J, Soerjomataram I, Dikshit R, Eser S, Mathers C, Rebelo M, Parkin DM, Forman D and Bray F: Cancer incidence and mortality worldwide: Sources, methods and major patterns in GLOBOCAN 2012. Int J Cancer 136: E359-E386, 2015.
4. Blaustein JD: Steroid hormone receptors: Long- and short-term integrators of the internal milieu and the external environment. Horm Metab Res 44: 563-568, 2012.
5. Nair S and Sachdeva G: Estrogen matters in metastasis. Steroids 138: 108-116, 2018.
6. Fan S, Liao Y, Liu C, Huang Q, Liang H, Ai B, Fu S and Zhou S: Estrogen promotes tumor metastasis via estrogen receptor beta-mediated regulation of matrix-metalloproteinase-2 in non-small cell lung cancer. Oncotarget 8: 56443-56459, 2017.
7. Chlebowski RT, Schwartz AG, Wakelee H, Anderson GL, Stefanick ML, Manson JE, Rodabough RJ, Chien JW, Wactawski-Wende J, Gass M, *et al*; Women's Health Initiative Investigators: Oestrogen plus progestin and lung cancer in postmenopausal women (Women's Health Initiative trial): A post-hoc analysis of a randomised controlled trial. Lancet 374: 1243-1251, 2009.
8. Garon EB, Siegfried JM, Stabile LP, Young PA, Marquez-Garban DC, Park DJ, Patel R, Hu EH, Sadeghi S, Parikh RJ, *et al*: Randomized phase II study of fulvestrant and erlotinib compared with erlotinib alone in patients with advanced or metastatic non-small cell lung cancer. Lung Cancer 123: 91-98, 2018.
9. Brown M and O'Reilly S: Innate immunity and Toll-like receptor signaling in the pathogenesis of scleroderma: Advances and opportunities for therapy. Curr Opin Rheumatol 30: 600-605, 2018.
10. Akira S, Uematsu S and Takeuchi O: Pathogen recognition and innate immunity. Cell 124: 783-801, 2006.
11. Janeway CA Jr and Medzhitov R: Introduction: The role of innate immunity in the adaptive immune response. Semin Immunol 10: 349-350, 1998.
12. Bhattacharya D and Yusuf N: Expression of toll-like receptors on breast tumors: Taking a toll on tumor microenvironment. Int J Breast Cancer 2012: 716564, 2012.
13. Anthoney N, Foldi I and Hidalgo A: Toll and Toll-like receptor signalling in development. Development 145: 145, 2018.
14. Chow SC, Gowing SD, Cools-Lartigue JJ, Chen CB, Berube J, Yoon HW, Chan CH, Rousseau MC, Bourdeau F, Giannias B, *et al*: Gram negative bacteria increase non-small cell lung cancer metastasis via Toll-like receptor 4 activation and mitogen-activated protein kinase phosphorylation. Int J Cancer 136: 1341-1350, 2015.
15. Li D, Jin Y, Sun Y, Lei J and Liu C: Knockdown of toll-like receptor 4 inhibits human NSCLC cancer cell growth and inflammatory cytokine secretion *in vitro* and *in vivo*. Int J Oncol 45: 813-821, 2014.
16. Harmey JH, Bucana CD, Lu W, Byrne AM, McDonnell S, Lynch C, Bouchier-Hayes D and Dong Z: Lipopolysaccharide-induced metastatic growth is associated with increased angiogenesis, vascular permeability and tumor cell invasion. Int J Cancer 101: 415-422, 2002.
17. Lv W, Chen N, Lin Y, Ma H, Ruan Y, Li Z, Li X, Pan X and Tian X: Macrophage migration inhibitory factor promotes breast cancer metastasis via activation of HMGB1/TLR4/NF kappa B axis. Cancer Lett 375: 245-255, 2016.
18. Rusch VW, Chansky K, Kindler HL, Nowak AK, Pass HI, Rice DC, Shemanski L, Galateau-Sallé F, McCaughan BC, Nakano T, *et al*; IASLC Staging and Prognostic Factors Committee, advisory boards, and participating institutions: The IASLC Mesothelioma Staging Project: Proposals for the M Descriptors and for Revision of the TNM Stage Groupings in the Forthcoming (Eighth) Edition of the TNM Classification for Mesothelioma. J Thorac Oncol 11: 2112-2119, 2016.
19. Tang H, Liao Y, Xu L, Zhang C, Liu Z, Deng Y, Jiang Z, Fu S, Chen Z and Zhou S: Estrogen and insulin-like growth factor 1 synergistically promote the development of lung adenocarcinoma in mice. Int J Cancer 133: 2473-2482, 2013.
20. Huang Q, Zhang Z, Liao Y, Liu C, Fan S, Wei X, Ai B and Xiong J: 17β-estradiol upregulates IL6 expression through the ERβ pathway to promote lung adenocarcinoma progression. J Exp Clin Cancer Res 37: 133, 2018.
21. Tang H, Liao Y, Chen G, Xu L, Zhang C, Ju S and Zhou S: Estrogen upregulates the IGF-1 signaling pathway in lung cancer through estrogen receptor-β. Med Oncol 29: 2640-2648, 2012.
22. Liu C, Liao Y, Fan S, Tang H, Jiang Z, Zhou B, Xiong J, Zhou S, Zou M and Wang J: G protein-coupled estrogen receptor (GPER) mediates NSCLC progression induced by 17β-estradiol (E2) and selective agonist G1. Med Oncol 32: 104, 2015.
23. Hernandez H, Medina-Ortiz WE, Luan T, Clark AF and McDowell CM: Crosstalk between transforming growth factor beta-2 and Toll-like receptor 4 in the trabecular meshwork. Invest Ophthalmol Vis Sci 58: 1811-1823, 2017.
24. Shaaban AA, El-Kashef DH, Hamed MF and El-Agamy DS: Protective effect of pristimerin against LPS-induced acute lung injury in mice. Int Immunopharmacol 59: 31-39, 2018.
25. Vinci M, Box C and Eccles SA: Three-dimensional (3D) tumor spheroid invasion assay. J Vis Exp 99: e52686, 2015.
26. Del Pozo JL: Primers on molecular pathways: Lipopolysaccharide signaling - potential role in pancreatitis and pancreatic cancer. Pancreatology 10: 114-118, 2010.
27. Siegfried JM and Stabile LP: Estrongenic steroid hormones in lung cancer. Semin Oncol 41: 5-16, 2014.
28. Matsunaga N, Tsuchimori N, Matsumoto T and Ii M: TAK-242 (resatorvid), a small-molecule inhibitor of Toll-like receptor (TLR) 4 signaling, binds selectively to TLR4 and interferes with interactions between TLR4 and its adaptor molecules. Mol Pharmacol 79: 34-41, 2011.
29. Thomas C and Gustafsson JA: The different roles of ER subtypes in cancer biology and therapy. Nat Rev Cancer 11: 597-608, 2011.
30. Weaver AM: Invadopodia: Specialized cell structures for cancer invasion. Clin Exp Metastasis 23: 97-105, 2006.
31. Saykali BA and El-Sibai M: Invadopodia, regulation, and assembly in cancer cell invasion. Cell Commun Adhes 21: 207-212, 2014.
32. Goertzen CG, Dragan M, Turley E, Babwah AV and Bhattacharya M: KISS1R signaling promotes invadopodia formation in human breast cancer cell via β-arrestin2/ERK. Cell Signal 28: 165-176, 2016.

33. Kovats S: Estrogen receptors regulate innate immune cells and signaling pathways. Cell Immunol 294: 63-69, 2015.
34. Mai CW, Kang YB and Pichika MR: Should a Toll-like receptor 4 (TLR-4) agonist or antagonist be designed to treat cancer? TLR-4: Its expression and effects in the ten most common cancers. Onco Targets Ther 6: 1573-1587, 2013.
35. Rich AM, Hussaini HM, Parachuru VP and Seymour GJ: Toll-like receptors and cancer, particularly oral squamous cell carcinoma. Front Immunol 5: 464, 2014.
36. Chiang AC and Massagué J: Molecular basis of metastasis. N Engl J Med 359: 2814-2823, 2008.
37. Alaseem A, Alhazzani K, Dondapati P, Alobid S, Bishayee A and Rathinavelu A: Matrix Metalloproteinases: A challenging paradigm of cancer management. Semin Cancer Biol 56: 100-115, 2019.
38. Brown GT and Murray GI: Current mechanistic insights into the roles of matrix metalloproteinases in tumour invasion and metastasis. J Pathol 237: 273-281, 2015.
39. Prossnitz ER and Barton M: The G-protein-coupled estrogen receptor GPER in health and disease. Nat Rev Endocrinol 7: 715-726, 2011.